

Interference effects in two-photon above-threshold ionization by multiple orders of high-order harmonics with random or locked phases

Eric Cormier,^{1,2} Anna Sanpera,^{1,3} Maciej Lewenstein,^{1,4} and Pierre Agostini¹

¹*Service des Photons, Atomes et Molécules, DRECAM, Centre d'Etudes de Saclay, F-91191 Gif-Sur-Yvette, France*

²*CELIA, Université de Bordeaux I, 351 Cours de la Libération, F-33405 Talence, France*

³*Departament de Física, Universitat Autònoma de Barcelona, 08193 Bellaterra, Spain*

⁴*Institut für Theoretische Physik, Universität Hannover, 30167 Germany*

(Received 9 November 1998)

We numerically study two-photon processes using a set of harmonics from a Ti:sapphire laser and, in particular, interference effects in the above-threshold ionization spectra. We compare the situation where the harmonic phases are assumed locked to the case where they have a random distribution. Suggestions for possible experiments, using realistic parameters, are discussed. [S1050-2947(99)04305-X]

PACS number(s): 32.80.Rm, 32.80.Qk

I. INTRODUCTION

High-order harmonic generation (HOHG) refers to the radiation emitted during the interaction of a short laser pulse with a gas jet. The spectrum of such a radiation consists of a series of odd harmonics of the fundamental frequency having approximately equal conversion efficiency (plateau), and followed by an abrupt cutoff. A complete description of harmonic generation which allows for a direct comparison with the experiments should include not only the response of the single atom to the laser field, but also the propagation of the different harmonics generated through the macroscopic medium. Recently, several studies on harmonic generation have focused on the properties of the phase of the generated harmonic waves, considering both single-atom and propagation effects [1]. Within the frame of the single-atom response the strength and the phase of each harmonic wave correspond to the modulus and the phase acquired by the dipole moment $d(t)$, or equivalently, the dipole acceleration induced by the external laser field. Thus the spectrum of the radiated harmonics can be directly calculated from the Fourier transform of the dipole acceleration [2]:

$$D(\omega) = \int \dot{d}(t) e^{i\omega t} dt = A(\omega) e^{i\phi(\omega)}, \quad (1)$$

where $A(\omega)$ is the amplitude, $\phi(\omega)$ is the phase of the dipole acceleration in the frequency domain, and $|D(\omega)|^2$ is the strength of the harmonics. The single-atom response shows that the phase of each harmonic, $\phi(\omega)$, is usually shifted with respect to the fundamental phase and depends strongly on the intensity of the laser field [3]. Let us recall that the harmonics are said to be phase locked if the phase of each individual harmonic is a linear function of its order q so it can be written as $\phi_q = \beta q \omega + \zeta$ where $\beta q \omega$ is the linear q -dependent term and ζ a constant term identical for all harmonics. In general, harmonics from the plateau region present a random phase when compared to each other, and only the harmonics from the cutoff region are locked in phase. This can be intuitively understood using the semiclassical description of the atom-field interaction in which harmonic generation results from the recombination of those

electrons which have previously tunneled out through the effective potential produced by the Coulomb and the laser field. The induced dipole, and hence the process of harmonic generation, corresponds to trajectories in which the electron returns to the core with appropriate kinetic energy and recombines, emitting a photon. Each contribution then contains a phase factor equal to the real part of the action acquired by the electron following the respective trajectory [3]. Among all possible trajectories, very few of them are relevant. For the harmonics in the cutoff there is only one dominant trajectory, corresponding to a single recombination time and, therefore, the phase of the harmonics in this region remains locked. On the other hand, for the harmonics lying in the plateau, there are typically two relevant trajectories corresponding to two different returning times. The phase of such a harmonic contains the contributions of these two trajectories and, in particular, their quantum interferences. This quantum interference term leads to an apparently random phase. In spite of this fact, when one analyzes the harmonic emission in time rather than in frequency domain, one observes a clear periodicity of the signal. Antoine *et al.* [4] have shown that the time-dependent emission consists of a train of ultrashort pulses with two dominant pulses per half cycle, each corresponding to one of the relevant trajectories. Further studies show that under certain geometrical conditions it should be possible to phase match the contribution of only one of these trajectories. That results in a train of ultrashort pulses equivalent to those obtained by combining several plateau harmonics with their phases locked.

From an experimental point of view, determining the relative phase of the emitted harmonics is not a straightforward task. Its study necessarily involves some type of interference effects between the different harmonics. Although some pioneering work on interference between harmonics of the same order has been recently reported [5–7], a conclusive result on the relative phase has not yet been achieved.

In this paper we address this question using a combination of successive odd harmonics to study two-photon processes. When several harmonics simultaneously irradiate an atom, there exist various paths associated with two-photon transitions ending up in the same final state thus leading to possible interference effects. Those effects should be clearly

present in the ionization rates, as well as in the photoelectron spectra. Similar effects of sensitivity to harmonics phases have been previously studied in a series of papers on above-threshold ionization (ATI) by mixing harmonics and infrared laser fields [8,9]. Furthermore, two-photon ionization of atoms with photons pertaining to the vacuum-ultraviolet–x-ray-ultraviolet domain have recently been reported for argon using the third harmonic of a KrF laser [10], and for helium using the ninth harmonic of a Ti:sapphire laser [11] thus giving evidence of its experimental feasibility. In this paper, we focus on two-photon ionization of atoms by Ti:sapphire harmonics whose order varies from $q=11$ to $q=33$.

Essentially, the aim of the paper is to show that measurable quantities such as ionization or the more detailed photoelectron spectrum have a different behavior depending on the relative phases of the harmonics and to study these effects quantitatively. The paper is organized as follows: in Sec. II we develop a combinatorial model derived from perturbation theory which is able to provide rough scaling laws for the total ionization rates as a function of the number of harmonics present in the field. Section III reports on numerical above-threshold ionization rates obtained by solving the time-dependent Schrödinger equation (TDSE) with realistic polychromatic pulses for atomic H. Section IV is a study of quasiresonant multiphoton ionization (MPI) in He^+ also obtained by solving TDSE. Finally, in Sec. IV we give concluding remark and we comment on possible experiments.

II. COMBINATORIAL MODEL

The model presented in this section provides an estimate for the ionization probability as a function of the number of successive odd harmonics included in the laser field. It is based on a combinatorial approach and a perturbative treatment of the atom-field interaction.

Let us first sketch the problem under investigation. We consider electrons emitted during ionization via a two-photon process from an atom initially in its ground state (the possible case where some excited intermediate states come into resonance with the absorption of only one photon is discussed in Sec. IV). Since the field considered here consists of a linear combination of successive odd harmonics:

$$E(t) = \sum_q E_q \cos(q\omega_L t + \phi_q), \quad (2)$$

photons of different energies will be involved in the production of electrons with different kinetic energies, as is illustrated in Fig. 1. Note that the energies at which electrons are released appear on the photoelectron spectrum separated exactly by the energy of two photons of the fundamental field (ω_L) which generates the harmonics. Moreover, electrons at a particular energy may have been released by the absorption of photons originated from distinct harmonics. The only restriction is that whatever the combination of photons is, the sum of their energies ought to be the same. For example, the production of electrons in the central peak of the electron spectrum of Fig. 1 results from transitions following three different quantum paths. The amplitudes associated to each quantum path may interfere depending on the relative phase of the photons involved. The interference pattern appears

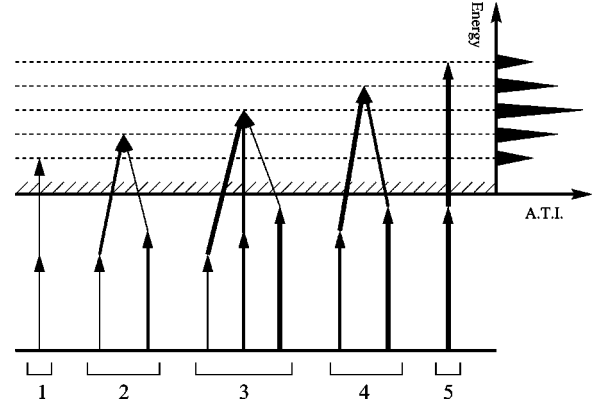


FIG. 1. Sketch of the processes investigated in the case of the mixing of three harmonics. Also shown is the corresponding electron spectrum.

clearly if one writes the ionization probability associated with these processes (labeled 3 in Fig. 1) within perturbation theory:

$$p_{fg} = |{}^a M_{fg}^{(2)} E_1 E_3 e^{i(\phi_1 + \phi_3)} + {}^b M_{fg}^{(2)} (E_2 e^{i\phi_2})^2 + {}^c M_{fg}^{(2)} E_3 E_1 e^{i(\phi_3 + \phi_1)}|^2, \quad (3)$$

where the subscripts 3, 1, and 2 refer to the biggest, the smallest, and the intermediate photon, E refers to the maximum field amplitude, and ϕ to the phase of the photons. The transition amplitude matrix elements from the initial state $|g\rangle$ to the final state $|f\rangle$ for the three paths are given by

$$\begin{aligned} {}^a M_{fg}^{(2)} &= \lim_{\epsilon \rightarrow 0} \sum_n \frac{\langle f|z|n\rangle \langle n|z|g\rangle}{\omega_g + \omega_1 - \omega_n + i\epsilon}, \\ {}^b M_{fg}^{(2)} &= \lim_{\epsilon \rightarrow 0} \sum_n \frac{\langle f|z|n\rangle \langle n|z|g\rangle}{\omega_g + \omega_2 - \omega_n + i\epsilon}, \\ {}^c M_{fg}^{(2)} &= \lim_{\epsilon \rightarrow 0} \sum_n \frac{\langle f|z|n\rangle \langle n|z|g\rangle}{\omega_g + \omega_3 - \omega_n + i\epsilon}, \end{aligned} \quad (4)$$

where the summation runs over all coupled intermediate states including the continuum. The special case of ATI can be numerically extrapolated [12] or computed accounting explicitly for the resonant free-free transition matrix elements [13]. Since we assume the interaction with a linearly polarized field and express it in the length gauge, only the matrix elements of z appear in expression (4). The ionization probability then reads

$$\begin{aligned} p_{fg} &= |{}^a M_{fg}^{(2)}|^2 E_1^2 E_3^2 + |{}^b M_{fg}^{(2)}|^2 E_2^4 + |{}^c M_{fg}^{(2)}|^2 E_3^2 E_1^2 \\ &+ ({}^a M_{fg}^{(2)} {}^c M_{fg}^{(2)} * + \text{c.c.}) E_1^2 E_3^2 \\ &+ ({}^a M_{fg}^{(2)} {}^b M_{fg}^{(2)} * E_1 E_3 E_2^2 * e^{i(\phi_1 + \phi_3 - 2\phi_2)} + \text{c.c.}) \\ &+ ({}^b M_{fg}^{(2)} {}^c M_{fg}^{(2)} * E_2^2 E_3^2 E_1^2 * e^{-i(\phi_1 + \phi_3 - 2\phi_2)} + \text{c.c.}). \end{aligned} \quad (5)$$

Interferences in the probability given by Eq. (5) are governed by the phase difference $\Delta = \phi_1 + \phi_3 - 2\phi_2$, that is, the relative phase between the harmonics involved in this process. Such a partial probability can be derived for all accessible final states. Note that interferences are always absent in processes involving fewer than three different photons, which is always the case for the processes leading to the two first and two last final states (like processes labeled 1, 2, 4, and 5 in Fig. 1) independently of the total number of harmonics included in the field.

When the incident field is a linear combination of successive harmonics, there exist several distinct quantum paths associated to transitions to the same final state. These paths may interfere depending on the relative phase between the photons. Obviously, the number of possible interfering paths increases with the number of different frequencies included in the field.

To simplify the problem, we will now assume that all harmonics have the same strength, that is, $E_1 = E_2 = E_3 = E$. As the harmonics we are considering here all come from the plateau part of the spectrum, this assumption is generally fulfilled. Furthermore, we also assume that all two-photon transition amplitude matrix elements [as they are defined in Eq. (4)] are real and have the same value, i.e., ${}^a M_{fg} = {}^b M_{fg} = {}^c M_{fg} = M$. Although never fulfilled in general, this approximation is reasonable if the first photon absorbed brings the system into a region free of intermediate resonances. For the case of our illustrative example, the ionization probability associated to the central process (labeled 3 in Fig. 1) corresponds to

$$p_{fg} = M^2 E^4 [5 + 4 \cos(\phi_1 + \phi_3 - 2\phi_2)]. \quad (6)$$

Let us now analyze the two configurations of harmonic phases we are interested in, that is, the phase-locked case and the random distribution of phases. As defined in the Introduction, if harmonics are phase locked to each other, their phase has the form $\phi_q = \beta q \omega + \zeta$. Applied to our example $\Delta = \phi_1 + \phi_3 - 2\phi_2$ simply reduces to zero. Therefore, the cosine function in Eq. (6) takes value one. On the other hand, we can interpret the random distribution of phases as a loss of coherence between different quantum paths. It is then reasonable to associate the random distribution to the average value of Eq. (6) over all possible phases. Since the average value of the cosine function is zero, all terms in the probability vanish except the constant (phase-independent) terms. Generalizing these results for an arbitrary number N of incident harmonics, we obtain that the ionization probability associated to the central peak behaves as

$$P_c^{(\text{PL})}(N) = \alpha^2 N^2 \quad (7)$$

and

$$P_c^{(\text{RP})}(N) = \alpha^2 \times \begin{cases} 2N-1 & \text{if } N \text{ odd} \\ 2N & \text{if } N \text{ even,} \end{cases} \quad (8)$$

where PL refers to phase-locked configuration, RP to random phase configuration, and $\alpha = ME^2$. The total two-photon ionization probability is straightforwardly obtained by integrating the electron spectrum over the electron energy range relative to the two-photon processes. This probability ac-

counts for the side peaks in the photoelectron spectrum and is obtained by simply adding the probability associated to each side peak (see Fig. 1). It can be shown that the total probabilities read

$$P^{(\text{PL})}(N) = \alpha^2 \left(2 \sum_{n=1}^{N-1} n^2 + N^2 \right) = \alpha^2 \left(\frac{2N^3}{3} + \frac{N}{3} \right) \quad (9)$$

and

$$P^{(\text{RP})}(N) = \alpha^2 \left(4 \frac{N(N-1)}{2} + N \right) = \alpha^2 (2N^2 - N). \quad (10)$$

As mentioned earlier, when ordered by increasing final state energy, the two first and two last processes will never show path interferences independently of the total number of harmonics involved. Also, the process having the largest number of interference terms will always be the central one (like process number 3 in Fig. 1).

To summarize, the total ionization associated with two-photon absorption should vary approximately as $2/3N^3$ if the harmonics are locked in phase, and as $2N^2$ if the relative phase between them is random. Accordingly, the ionization rate associated to the central process should vary as N^2 in the phase-locked case and as $2N$ if the phase distribution is random.

We expect that similar scaling properties will characterize other processes of interest, such as two-photon above-threshold ionization, which we shall discuss in the next section. The advantage of studying ATI instead of two-photon ionization processes is that such processes are free from intermediate resonances that modify the interference pattern, as we shall discuss in Sec. IV. The disadvantage, on the other hand, is that the ATI signal might be low and, consequently, the effects due to the relative phase of the harmonics might be difficult to observe experimentally.

Finally, it is worth stressing here that the problem considered in this section has a lot in common with the problems of ionization by stochastic laser fields, discussed in the literature in the 1970s and 1980s [14]. In particular, the enhancement by a factor $K!$ of the K -photon ionization probability by multimode laser fields has been predicted and observed. In our random phase model, the same effect is responsible for the fact that $P^{(\text{RP})} \approx 2!N^2$. On the other hand, the problem considered in this paper is more general and deals with the differences induced by random and phase-locked configurations in laser pulses in *real* atoms, i.e., it fully accounts for atomic bound states and continuum structures.

III. TWO-PHOTON ABOVE-THRESHOLD IONIZATION

In this section, ATI is investigated using a time-dependent nonperturbative approach. It consists in solving the time-dependent Schrödinger equation for a hydrogen atom interacting with the combination of several harmonic fields. The method used to solve the TDSE and to compute the electron spectrum is based on the expansion of the total wave function on spherical harmonics and B -spline functions (see [15]). The temporal propagation in the length gauge is well adapted to the rather low intensities considered here. The

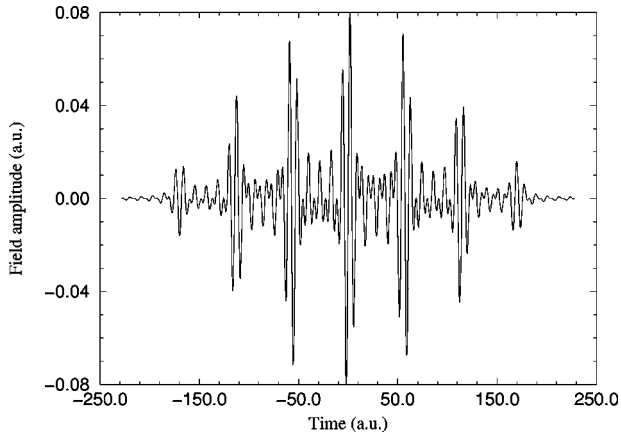


FIG. 2. Electromagnetic field amplitude corresponding to a linear combination of five odd harmonics ranging from order 11 to 19 ($\hbar\omega_L = 1.5$ eV).

electron spectra correspond to electrons emitted in the direction of the polarization.

A. Ionization of hydrogen in its ground state

We have computed the electron spectra obtained by shining a linear combination of successive harmonics on atomic hydrogen in its ground state. The frequencies of the selected harmonics are chosen so that absorption of a single photon already brings the system into the continuum. Thus, the two-photon processes we are interested in belong to the so-called above-threshold ionization regime. In our approach, the field is described semiclassically as

$$E(t) = E_0 f(t) \sum_{n=1}^N \cos(q\omega_L t + \phi_q), \quad q = 2(n-1) + q_0, \quad (11)$$

where $f(t)$ is the normalized envelope of the field, in our case a cosine squared with 5 fs full width at half maximum (20 cycles of harmonic 11); E_0 is the maximum field amplitude (identical for all harmonics) corresponding to an intensity of 10^{13} W/cm²; $\hbar\omega_L = 1.5$ eV is the fundamental photon energy, and q_0 indicates the lowest harmonic component in the polychromatic field. The number of harmonics we consider varies from $N=2$ to $N=5$, so that the odd harmonics included are $H13-H15$ for $N=2$, $H13-H17$ for $N=3$, $H11-H17$ for $N=4$, and $H11-H19$ for $N=5$. The field corresponding to the case $N=5$ is plotted in Fig. 2. The electron spectrum due to such a field is shown in Fig. 3 where we observe that electrons produced via different order processes are clearly distinguishable. The spectrum has to be read as follows: there are three clear subsets of ATI peaks, each of them corresponding to a different order process. The left-most subset corresponds to order 1, that is, direct photoionization via the absorption of a single photon ($H11$ for the very first peak and $H19$ for the fifth). The second subset, which is the one investigated here, embodies all processes of order 2. For example, the third peak of that subset results from the simultaneous absorption of either two photons from the harmonic 13, or one from the harmonic 11 and another from the harmonic 15. All possible allowed polychromatic combinations are included in this type of simulation. Higher-

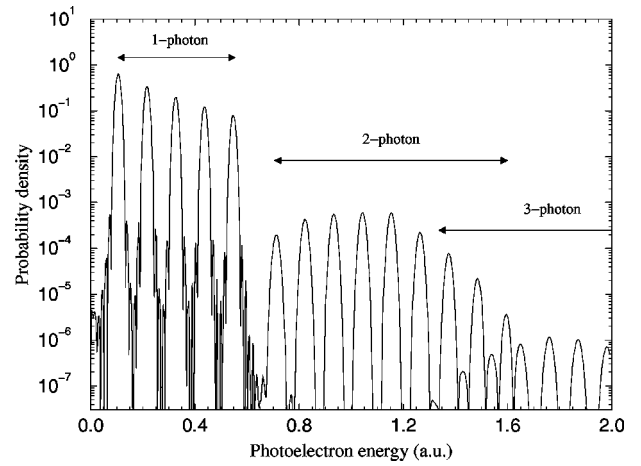


FIG. 3. ATI spectrum of H(1s) ionized by the selection of harmonics defined in Fig. 2. The three different subsets of ATI peaks correspond to different orders of processes.

order processes appear with exponentially decreasing probability and, therefore, their study has a restricted interest from an experimental point of view.

We have limited ourselves to a maximum of five combined harmonics in this study because higher values would lead to overlapping subsets of ATI peaks as is almost the case for $N=5$ where the three-photon process subset partly overlaps the two-photon subset (see Fig. 3).

Let us now focus on the two-photon above-threshold ionization, that is, the central subset of ATI peaks in Fig. 3. The problem of interest here is to determine how much the total ionization associated with two-photon absorption increases as we increase the number of harmonics in the field assuming that either all harmonics are locked in phase, or their relative phases are random.

We have first simulated the case of phase-locked harmonics. This is achieved by solving the TDSE when all harmonic phases ϕ_q are set to zero. Figure 4 shows the two-photon ionization probability as a function of the number of harmonics included in the field. The main result to be read from Fig.

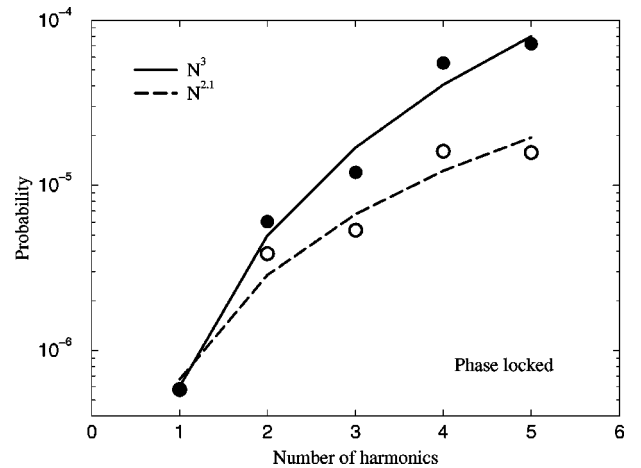


FIG. 4. Two-photon ATI total probability (filled circles) and two-photon ATI probability restricted to the central peak (open circles) as a function of the number of harmonics N for the locked phase case. The line and dashed line are power law fitting curves with a respective argument of 3 and 2.1.

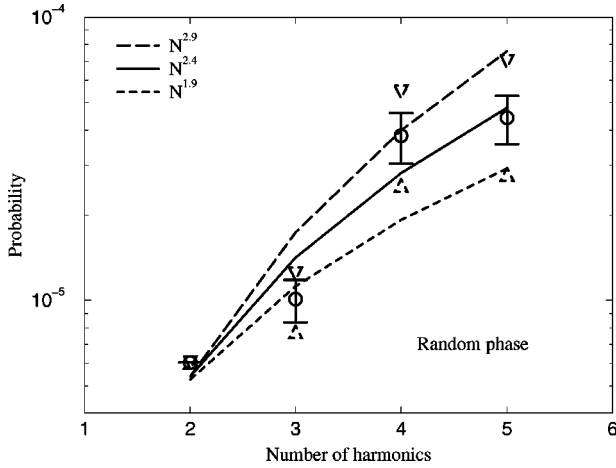


FIG. 5. Two-photon ATI total probability statistics (500 runs) as a function of N . The relative phases are random. Open circles refer to the average value of the distribution (power law fit with an argument of 2.4). Also shown are the maximum, minimum values of the distribution and the standard deviation (triangles down, up, and error bars, respectively).

4 is that ionization certainly scales as the cubic power of the number of harmonics as predicted by the combinatorial approach, Eq. (9). Similarly, the ionization probability associated with the central ATI peak scales as $N^{2.1}$, in good agreement with Eq. (7).

To simulate the case where the phases are random, we have accumulated the results of 500 different random phase configurations after solving the Schrödinger equation for each of them and we have averaged the results at the end. This has been done for each value of N . We report in Fig. 5 the ionization probability thus obtained together with its statistical fluctuations. The most interesting result here is the behavior of the average value of the ionization (open circles in Fig. 5). The average value scales as $N^{2.4}$, departing significantly from the combinatorial estimate that predicts an N^2 law [Eq. (10)]. Let us now examine the statistical fluctuations. On the one hand, we find that the maximum value of the ionization (down triangles in Fig. 5) scales as $N^{2.9}$, very close to that of the phase-locked case. Obviously, the configurations that lead to such maximal value are the special cases where all phase differences are close to zero as in our simulation of the phase-locked configuration. On the other hand, the most globally destructive phase configuration leading to the minimum value of the ionization probability scales as $N^{1.9}$ (up triangles in Fig. 5). We have also investigated the ionization probabilities associated to the central two-photon ATI peak, since it is the transition that involves the largest number of interfering quantum paths. The results are presented in Fig. 6. The average value of the ionization probability scales as ($N^{0.7}$) in comparison with the fit ($N^{2.1}$) obtained for the phase-locked case. Finally, its minimum value drops dramatically since interferences now can be completely destructive, that is, there exists a particular configuration of phases able to totally suppress ionization for this particular electron energy. This feature is absent in the case of total two-photon ionization since, as explained before, the four outermost ATI peaks correspond to transitions involving only two quantum paths, and therefore are not affected by any change in phase.

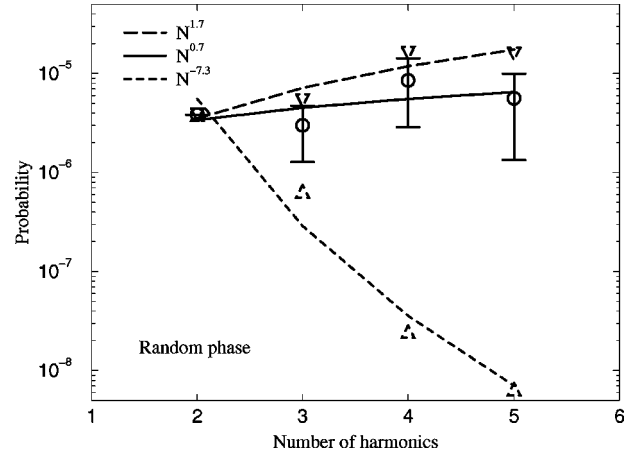


FIG. 6. Same as Fig. 5 but restricted to the central peak. Open circles: average value. The power law fit gives an argument of 0.7.

A way to improve the statistical results is to increase the number of harmonics included in the field by using higher-order harmonics. This will prevent us from having different ATI order processes overlapping but also the ionization signal will decrease because the cross section associated to these processes decays with increasing photon energy.

B. Ionization of hydrogen in the 2s state

A solution to ease two-photon ionization due to higher harmonics is to start from a less bound atomic energy level, such as $H(2s)$, for example.

By choosing harmonic 21 ($\hbar\omega_L = 1.5$ eV) as the central component, we can combine up to seven harmonics. Because of the lower binding energy, we now set the field intensity of all harmonic components to 10^{10} W/cm². As expected with this intensity, the probability for ionization by a two-photon process is very low. However, one should keep in mind that this probability varies as I^2 in agreement with the process order, and that the intensity we are using here underestimates experimental attainable fluxes.

We find that in the phase-locked case, the scaling laws concerning total ionization associated with two-photon absorption shown in Fig. 7 agree very well with the combinatorial estimates expressed in Eqs. (7) and (9).

The random phase simulation for $H(2s)$ has been carried out by accumulating results from 300 resolutions of the TDSE, each time with a new random distribution of harmonic phases. In Fig. 8, we show the two-photon ATI probability, obtained by integrating the spectrum over the whole range of electron energies corresponding to two-photon ATI processes. In the case $N=7$, the integration runs from $E_k = 40$ eV up to $E_k = 76$ eV. Here again, there is a significant departure of the average value of the ionization probability, which scales as $N^{2.55}$, from the N^2 combinatorial law associated with the random phase configuration.

Finally, as in the preceding section, we have looked at the most phase sensitive ATI peak located at the center of the two-photon ATI subset in the electron spectrum. The expected combinatorial power laws are 2 and 1 for harmonic phases, locked and random, respectively. The quantum mechanical computation gives the values of 2 and 1.3 for the respective configurations as is shown in Fig. 9. The lower

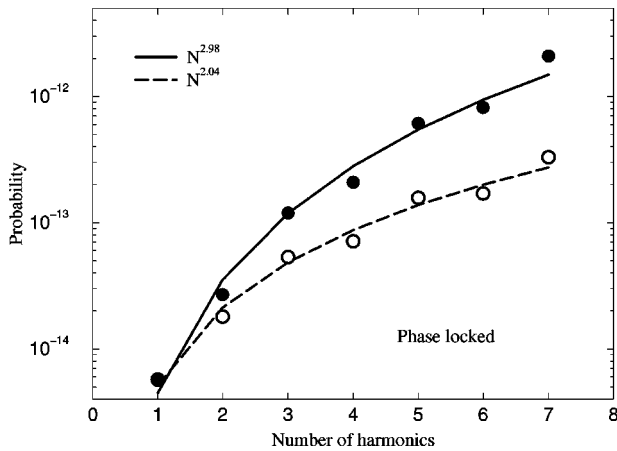


FIG. 7. Ionization from $H(2s)$: Two-photon ATI total probability (filled circles) and two-photon ATI probability restricted to the central peak (open circles) as a function of N . The relative phases are locked (zero). The line and dashed line are power law fitting curves with a respective value of 2.98 and 2.04.

limit of the distribution drops abruptly until it reaches the background induced by the numerical accuracy (around 10^{-16} in Fig. 9).

To summarize, we have shown that there is a different behavior in the two-photon ionization probabilities as a function of N if one considers the harmonics locked in phase or if the distribution of their phases is random. To a rough extent, scaling laws can be explained using the idealized combinatorial model of Sec. II.

IV. TWO-PHOTON IONIZATION

The preceding section has been devoted to the study of two-photon ATI processes, where absorption from a single photon already brings the system into the continuum. Now, we propose to study direct two-photon harmonic ionization (MPI). In contrast with the two-photon ATI cases, ionization now requires two harmonic photons, so the interference effects governed by the harmonic phases appear directly in the

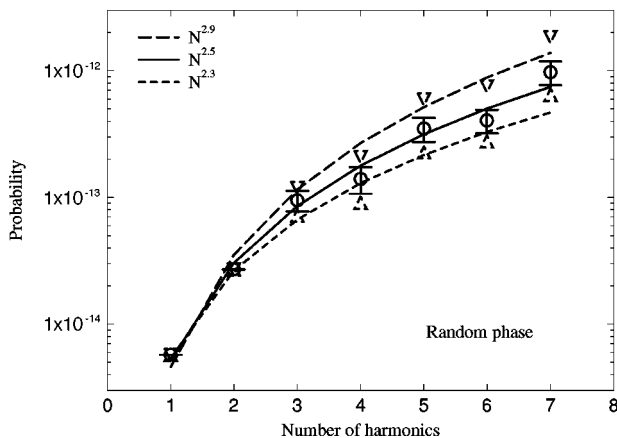


FIG. 8. Ionization from $H(2s)$: Two-photon ATI total probability statistics (300 runs) as a function of N . The relative phases are random. Open circles refer to the average value. The power law fit gives an argument of 2.5. Also shown are the maximum, minimum values and the standard deviation (triangles down, up, and error bars).

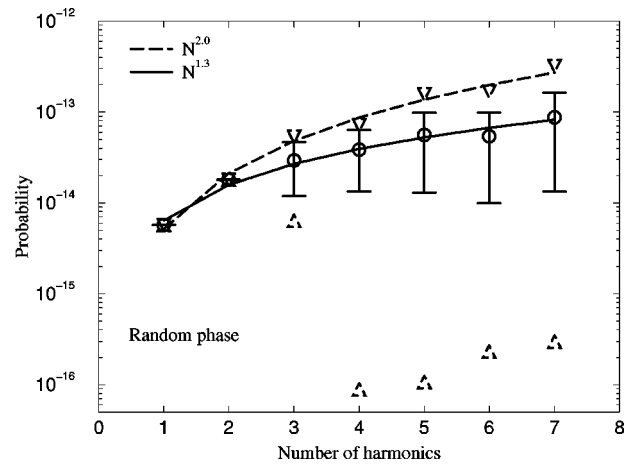


FIG. 9. Same as Fig. 8 but restricted to the central peak. Open circles: average value. The power law fit gives an argument of 1.3.

first subset of peaks in the electron spectra.

At this point, let us recall that our combinatorial model is based on the assumption that the total transition amplitude towards a given final state is only related to the number of interfering paths leading to such a final state. This assumption, in turn, implies that all the matrix elements involved in the transitions are considered equal. The results obtained so far indicate that this is a reasonable assumption for two-photon ATI processes where bound-bound transitions do not play any essential role. However, two-photon ionization processes (MPI) may involve quasis resonant bound-bound transitions. At low intensities, i.e., in the frame of perturbation theory, the values of the bound-bound transition matrix elements depend strongly on how close the transition is from a resonance. As we shall see, this fact substantially modifies the results we have encountered so far.

In order to optimize the study of the interferences between different harmonics having, at the same time, a good control of the role of the resonances involved, we choose as a model a hydrogenic ion (He^+). Note, however, that the results we present in this section can be straightforwardly generalized to any atom or ion and, therefore, have a certain generic validity.

We numerically solve the TDSE for direct two-photon ionization, where the external field is a linear combination of different harmonic fields, all of them with the same polarization and intensity. As in the previous sections, we consider harmonics from a Ti:sapphire laser ($\hbar\omega_L = 1.5$ eV), set the intensity of each harmonic to 1.2×10^{12} W/cm², and calculate ionization probabilities as well as photoelectron spectra for phase-locked and random phase configurations. For our choice of parameters, the smallest harmonic from Ti:sapphire required for two-photon detachment of He^+ is the 19th and the largest one the 35th. Larger harmonics will directly detach the ion, and smaller ones than the 19th cannot achieve two-photon detachment.

Before proceeding further, it is illustrative to show some of the effects due to atomic resonances in the photoelectron spectrum. To this aim we display the spectrum for a phase-locked configuration containing (a) $N=4$ harmonics ranging from 19th to 25th (Fig. 10) and (b) $N=6$ harmonics ranging from 19th to 29th (Fig. 11). In both spectra there are two distinguishable sets of peaks: the first one corresponds to

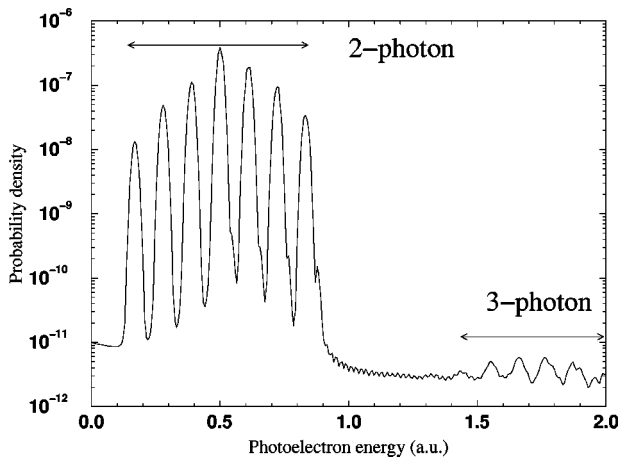


FIG. 10. Photoelectron spectrum of He^+ for a phase-locked configuration containing four harmonics (from 19th to 25th). The first subset corresponds to direct two-photon ionization processes. At higher energies a second subset of peaks corresponding to three-photon process appears.

two-photon detachment processes, the second one corresponds to three-photon processes (ATI peaks). From an experimental point of view, interest in the second subset should be restricted due to the low probability of three-photon processes.

The first subset contains $2N-1$ different peaks, where N is the number of harmonics present in the external field. As mentioned in the previous sections, the central peak of this subset corresponds, in both cases, to the transition involving the largest number of different quantum paths. While in Fig. 10 this peak is the most probable one, in Fig. 11 the central peak is clearly suppressed in comparison with lower-order peaks. The reason for this peak suppression is due to the fact that the 27th harmonic [only present in case (b)] crosses the $1s-2p$ resonance quasiresonantly.

Let us now focus on the results corresponding to ionization probabilities. As in Sec. III, the two-photon detachment probability is calculated by integrating the area below all two-photon processes in the photoelectron spectrum. We

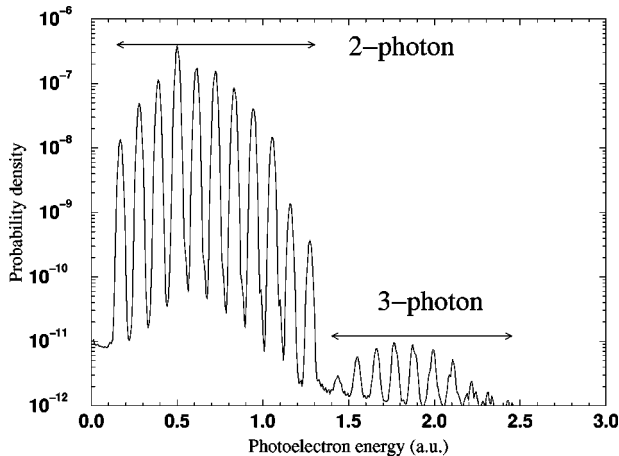


FIG. 11. Same as Fig. 10 but for an external field containing now six harmonics components (from 19th to 29th). Observe that the peak distribution in the two-photon ionization processes does not follow the same pattern as before.

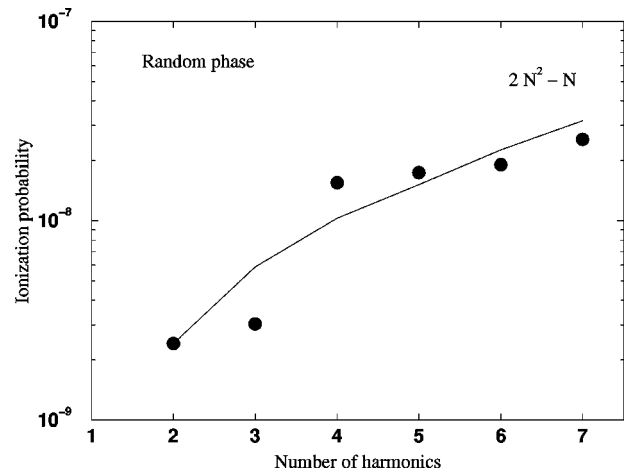


FIG. 12. Average value of the ionization probability versus the number of harmonic components for random phase configuration. Full line corresponds to the combinatorial estimate [Eq. (10)] and dots display the numerical results.

start by analyzing the random phase configuration where we have accumulated results from a large number of random phase distributions and we have averaged them at the end. In Fig. 12 we plot the average value of the ionization probability versus the number of incident harmonics N which varies from $N=2$ to $N=7$. The lowest harmonic involved is always the 19th so $N=2$ includes harmonics 19-21, $N=3$ includes harmonics 19-21-23, and so on. The overall behavior of the ionization probability obtained numerically (dots) agrees relatively well with the combinatorial approach (full line).

In Fig. 13 we present the corresponding ionization probability as a function of the number of harmonics N , for the phase-locked configuration. In the simulation, all the individual harmonic phases, ϕ_q , have been set to zero. Again, the full line represents the results from the combinatorial approach [Eq. (9)], while symbols show our numerical results. We observe that for low-order incident harmonics, i.e., from the 19th to the 25th, the numerical results agree relatively well with the combinatorial approach. However, when higher harmonics are included (from the 27th onwards) the combinatorial approach clearly overestimates the ionization

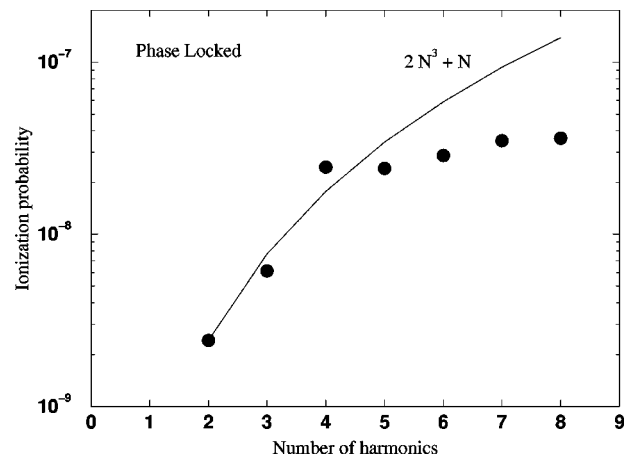


FIG. 13. Same as Fig. 12 but for a locked phase configuration. Full line corresponds to the combinatorial estimate [Eq. (9)] and dots display the numerical results.

TABLE I. Two-photon transition matrix elements as a function of the order of each photon.

Matrix elements: $s \rightarrow p \rightarrow d$							
	19	21	23	25	27	29	31
19	-84.1	-66.1	-58.2	-49.1	-41.8	-35.8	-30.9
21	-90.5	-74.4	-61.9	-52.0	-44.2	-37.9	-32.7
23	-105.4	-86.2	-71.4	-59.9	-50.8	-42.7	-37.5
25	-168.1	-136.4	-112.4	-94.0	-79.5	-68.0	-58.6
27	132.1	105.1	85.3	70.5	59.1	50.2	43.1
29	-20.6	-19.9	-16.9	-14.5	-12.5	-10.9	-9.5
31	-183.0	-151.7	-125.3	-105.2	-89.5	-76.8	-66.6

probability obtained numerically. The discrepancy between the estimate and the numerical value then becomes dramatic.

This discrepancy can be understood by analyzing the role of resonances within perturbation theory. Under the parameters we have used in the simulations, the energy of the 27th harmonic is slightly detuned (from above) from the $1s-2p$ resonance. As a result, the matrix elements corresponding to transitions of the type

$$M \propto \sum_n \frac{\langle f|z|n\rangle\langle n|z|1s\rangle}{\omega_{1s} + \omega_{27} - \omega_n} E_{27}^* E_i, \quad (12)$$

where i refers to the second photon absorbed, flip their sign compared to those transitions which are far off resonance.

Let us analyze in more detail the two-photon MPI transitions. From the two possible paths starting from the ground state leading to photodetachment, $s \rightarrow p \rightarrow s$ and $s \rightarrow p \rightarrow d$, the second one clearly dominates over the first one. This is because transitions that increase their principal quantum number and their angular momentum in the same direction are always favored compared to the others [16]. Therefore, we focus on two-photon transitions of the type $s \rightarrow p \rightarrow d$ and present the values of M in Table I.

The table has to be interpreted as follows: rows refer to the first absorbed photon and columns to the second one. For example, the first row displays the values of the matrix elements corresponding to transitions in which the first absorbed photon is the 19th harmonic and the second one the one indicated by the column label, i.e., transition amplitude of the type $\sum[\langle f|z|n\rangle\langle n|z|1s\rangle/(\omega_{1s} + \omega_{19} - \omega_n)]E_{19}E_i$.

As it should be, we observe that the values of the matrix elements (i) decrease as the energy of the final state increases and (ii) decrease for transitions far from resonances. Immediately after a resonance has been crossed, the matrix element flips its sign. Thus, with the parameters we have used in the simulation, all matrix elements corresponding to the absorption from the ground state of a photon from the 27th harmonic [Eq. (12)] flip their sign compared to all the other matrix elements shown in the table.

This relative sign flip strongly affects the total ionization probability in the phase-locked case, for which $P^{(PL)} \propto |\sum M_i|^2$, i.e., proportional to the square of the sum of the

individual matrix elements. It also has consequences for random phase configurations but there the effects are less dramatic. It is easier to understand the difference between both cases with an example. Consider an incident field containing harmonics 25, 27, and 29. Such an incident field leads to five possible final electron energy states, which, ordered by increasing energy, correspond to (i) 25+25 (absorption of two photons from harmonic 25); (ii) 25+27, 27+25; (iii) 25+29, 27+27, 29+25; (iv) 27+29, 29+27, and finally (v) 29+29. Remember that in order to have interference effects we need at least three different quantum paths contributing to the process. Therefore, the partial ionization probabilities associated to states (i), (ii), (iv), and (v) are the same regardless of the relative phase of the harmonics. The partial ionization probability associated to state (iii) which contains contributions from three different quantum paths depends on the relative phases of the harmonics. For phase-locked harmonics, it is proportional to $|M_{(25+29)} + M_{(27+27)} + M_{(29+25)}|^2$. On the other hand, if the harmonics have a random phase, the partial ionization probability associated to the final state (iii) is proportional to $|M_{(25+29)} + M_{(29+25)}|^2 + |M_{27+27}|^2$. Comparing both expressions, we note that it is only in the phase-locked case where the sign of $M_{(27+27)}$ plays a definite role since it acts effectively as a destructive interference term. Notice that the values of the matrix elements corresponding to transitions 27+25 and 27+29 do modify the partial ionization probabilities associated to the final states (ii) and (iv), respectively, but they do it exactly in the same way for both cases: locked and random phase configurations.

To corroborate our findings we have extended our numerical results up to the 33rd harmonic ($N=8$). For the parameters we have used, the photon energy of harmonic 33 is slightly higher than the atomic transition $1s \rightarrow 3p$. Consequently, the matrix elements corresponding to absorption from the ground state of a photon from harmonic 33 will again flip their sign, and again act as an effective destructive interference for locked phase configurations. As a result, the disagreement between the ionization probability and the combinatorial estimate should increase. Our numerical results support this conclusion.

In spite of the discrepancy between our numerical results and the combinatorial estimates, it should be stressed here that nevertheless the overall behavior of the ionization probability for random and phase-locked configurations remains distinct, allowing in principle for a distinction between both cases.

We would like to remark here that according to what we have seen, it might also occur that for a *particular* final state energy, its associated partial transition probability becomes larger for incident harmonics with random phases than for phase-locked harmonics. Such a partial peak inversion demonstrates that the effects due to atomic resonances can in some cases be strong enough to compensate the effects due to quantum phase interference.

To summarize, we have shown that the overall behavior of the ionization probability clearly depends on the relative phase configuration of the incident harmonics. Furthermore, we have shown that for phase-locked configurations and incident harmonic fields near resonance, the total ionization probability strongly departs from the combinatorial estimate and it no longer follows the N^3 power law [Eq. (9)]. If, on

the contrary, the incident harmonics are all far from atomic resonances, the combinatorial estimate accurately predicts the exact results [Eqs. (9) and (10)]. We stress, however, that most two-photon ionization experiments involving a set of harmonics are bound to show the effects of resonances. Finally, for incident harmonics with random phases, the average value of the ionization probability agrees relatively well with the combinatorial approach, i.e., N^2 .

V. CONCLUSIONS

In conclusion, we have shown that in two-photon ATI of hydrogen atoms by multiple orders of high-order harmonics, measurable quantities such as the ionization yield or the photoelectron spectra significantly depend on the relative phase of the harmonics. It should therefore be possible to determine experimentally the phase configuration of the high harmonics and, in particular, if the phases are locked. The method suggested by the calculation is a measurement of these quantities as a function of the number of selected harmonics. Clearly this is a difficult task. One difficulty lies in the relatively low photon harmonic flux currently achievable: 10^9 photons using 100 fs lasers in argon, and 10^7 photons using 30 fs in neon [1]. Such a flux is in general too low to

observe two-photon processes. However, several possibilities to increase the harmonic fluxes are under investigation, based on shortening the duration of the pump pulses [1,2,17] or improving the phase matching [20]. Furthermore, initial states prepared as coherent superpositions of two or more bound states can potentially increase the harmonic generation efficiency in the part of the spectrum we are interested in [18,19]. Another challenge to be faced in a real experiment will be the making of multilayer mirrors with different bandwidths to vary the number of selected harmonics without changing their relative phases. In spite of these obstacles, we think that such an experiment is not out of reach and could be useful in asserting the existence of subfemtosecond harmonic pulses in the cases of locked phases.

ACKNOWLEDGMENTS

A.S. would like to thank Richard Taïeb for very illuminating ideas concerning Sec. IV and acknowledges financial support from DGICYT (Spain) Contract No. PB95-0778-C02-02 and the European TMR program (Contract No. FMRX-CT96-0080). E.C. thanks Pascal Salières for a careful reading of the manuscript and P. Lambropoulos for clarifying discussions.

-
- [1] For a recent review see P. Salières, A. L'Huillier, P. Antoine, and M. Lewenstein, *Adv. At. Mol. Opt. Phys.* **41**, 83 (1999).
- [2] K. J. Schafer and K. C. Kulander, *Phys. Rev. Lett.* **78**, 638 (1997).
- [3] M. Lewenstein, P. Salières, and A. L'Huillier, *Phys. Rev. A* **52**, 4747 (1995).
- [4] P. Antoine, A. L'Huillier, and M. Lewenstein, *Phys. Rev. Lett.* **77**, 1234 (1996).
- [5] R. Zerne, C. Altucci, M. Bellini, M. Gaarde, T. W. Hänsch, A. L'Huillier, C. Lyngå, and C. G. Wahlström, *Phys. Rev. Lett.* **79**, 1006 (1997).
- [6] T. Ditmire and R. Smith, *Opt. Lett.* **23**, 618 (1998).
- [7] M. Bellini, C. Lyngå, A. Tozzi, M. Gaarde, T. W. Hänsch, A. L'Huillier, and C. G. Wahlström, *Phys. Rev. Lett.* **81**, 297 (1998).
- [8] V. Veniard, R. Taïeb, and A. Maquet, *Phys. Rev. Lett.* **74**, 4161 (1995).
- [9] V. Veniard, R. Taïeb, and A. Maquet, *Phys. Rev. A* **54**, 721 (1996).
- [10] D. Xenakis, O. Faucher, D. Charalambidis, and C. Fotakis, *J. Phys. B* **29**, L457 (1996).
- [11] Y. Kobayashi, T. Sekikawa, Y. Nabekawa, and S. Watanabe, *Opt. Lett.* **23**, 64 (1998).
- [12] E. Cormier and P. Lambropoulos, *J. Phys. B* **28**, 5043 (1995).
- [13] E. Cormier, H. Bachau, and J. Zhang, *J. Phys. B* **26**, 4449 (1993).
- [14] See, for instance, B.W. Shore, *The Theory of Coherent Atomic Excitation* (J. Wiley & Sons, New York, 1990), Vol. 2.
- [15] E. Cormier and P. Lambropoulos, *J. Phys. B* **29**, 2667 (1996).
- [16] H. A. Bethe and E. E. Salpeter, *Quantum Mechanics of One and Two Electron Atoms* (Academic, New York, 1998).
- [17] Z. H. Chang, A. Rudquist, H. Wang, M. Murnane, and H. Kapteyn, *Phys. Rev. Lett.* **79**, 2967 (1997); P. Salières, P. Antoine, and M. Lewenstein, *ibid.* **81**, 5544 (1998).
- [18] J. Watson, A. Sanpera, X. Chen, and K. Burnett, *Phys. Rev. A* **53**, R1962 (1996).
- [19] A. Sanpera, J. Watson, M. Lewenstein, and K. Burnett, *Phys. Rev. A* **54**, 4320 (1997).
- [20] A. Rundquist, C. G. Durfee III, Z. Chang, C. Herne, M. M. Murnane, and H. C. Kapteyn, *Science* **280**, 1412 (1998).